



GLOBAL JOURNAL OF RESEARCHES IN ENGINEERING: A
MECHANICAL AND MECHANICS ENGINEERING
Volume 14 Issue 2 Version 1.0 Year 2014
Type: Double Blind Peer Reviewed International Research Journal
Publisher: Global Journals Inc. (USA)
Online ISSN: 2249-4596 & Print ISSN: 0975-5861

Study of Viscous Dissipation on Natural Convection in a Vertical Conical Annular Porous Medium

By N. Ameer Ahmad & M. Ayaz Ahmad

University of Tabuk, Saudi Arabia

Abstract- In this paper, we study the heat transfer by Natural convection in a saturated porous medium including viscous dissipation in a vertical conical annular porous medium. Finite Element Method (FEM) has been used to solve the governing partial differential equations. Results are presented in terms of average Nusselt number (\overline{Nu}), streamlines and isothermal lines for various values of Rayleigh number (Ra), Cone angle (C_A), Radius ratio (R_r) and Viscous dissipation(ϵ).

Keywords: viscous dissipation (ϵ), rayleigh number (ra), cone angle (ca) and radius ratio (rr).

GJRE-A Classification : FOR Code: 091399p



Strictly as per the compliance and regulations of:



Study of Viscous Dissipation on Natural Convection in a Vertical Conical Annular Porous Medium

N. Ameer Ahmad^α & M. Ayaz Ahmad^σ

Abstract- In this paper, we study the heat transfer by Natural convection in a saturated porous medium including viscous dissipation in a vertical conical annular porous medium. Finite Element Method (FEM) has been used to solve the governing partial differential equations. Results are presented in terms of

average Nusselt number (\overline{Nu}), streamlines and isothermal lines for various values of Rayleigh number (Ra), Cone angle (C_A), Radius ratio (R_r) and Viscous dissipation (ϵ).

Keywords: viscous dissipation (ϵ), rayleigh number (ra), cone angle (c_a) and radius ratio (r_r).

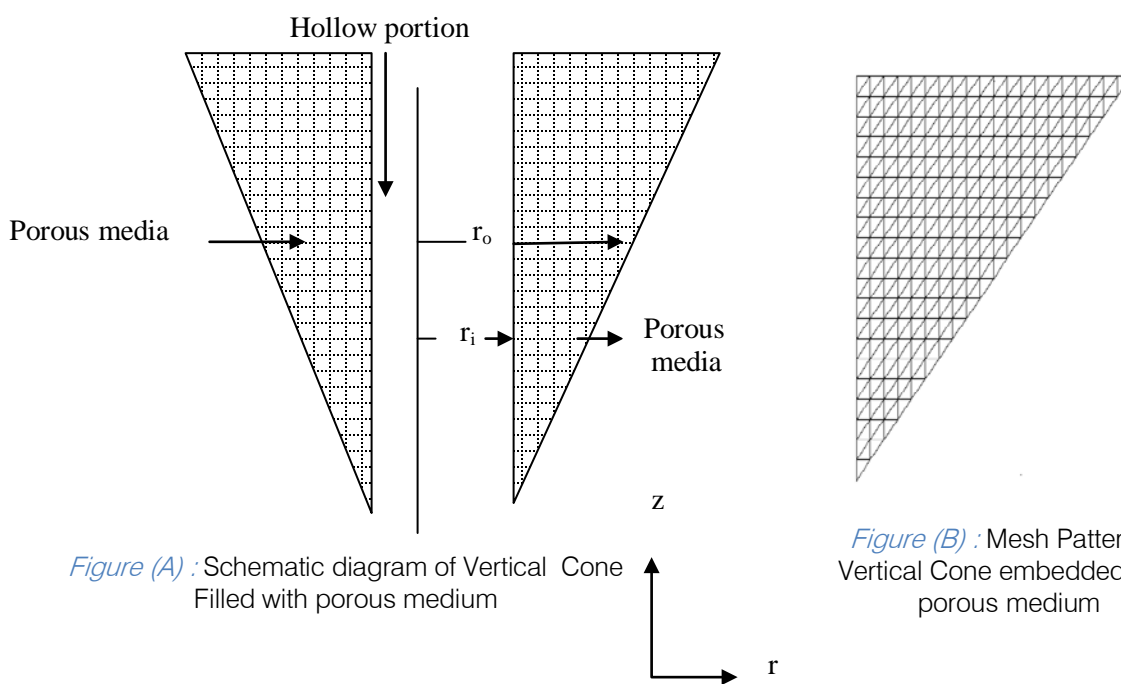


Figure (A) : Schematic diagram of Vertical Cone Filled with porous medium

Figure (B) : Mesh Pattern of Vertical Cone embedded with porous medium

NOMENCLATURE

a) List of Symbols

C_A Cone Angle

C_p Specific heat

D_p Particle diameter

g Gravitational acceleration

H_t Height of the vertical annular cone

K Permeability of porous media

P Pressure

\overline{Nu} Average Nusselt number

q_t Total heat flux

r, z Cylindrical co-ordinates

\bar{r}, \bar{z} Non-dimensional co-ordinates

r_i, r_o Inner and outer radius

Ra Rayleigh number

R_r Radius ratio

R_d Radiation parameter

Author α : Department of Mathematics, Faculty of Science, P.O. Box 741, University of Tabuk, Zip. 71491, Kingdom of Saudi Arabia. e-mail: n.ameer1234@gmail.com

Author σ : Department of Physics, Faculty of Science, University of Tabuk, Tabuk, KSA.

T	Temperature
\bar{T}	Non-Dimensional Temperature
u	Velocity in r direction
w	Velocity in z direction
b) Greek Symbols	
α	Thermal diffusivity
β_T	Co-efficient of thermal expansion
ε	Viscous dissipation parameter
ΔT	Temperature difference
σ	Stephan Boltzman constant
ρ	Density
γ	Coefficient of Kinematic viscosity
μ	Coefficient of dynamic viscosity
ϕ	Porosity
ψ	Stream function
$\bar{\psi}$	Non-dimensional stream function
c) Subscripts	
w	Wall
∞	Conditions at infinity
h	Hot
c	Cold
t	Total

I. INTRODUCTION

Natural convection flow and heat transfer in a saturated porous media has gained much attention during the past two decades because of its wide range of applications in packed bed reactors, porous insulation, beds of fossil fuels, nuclear waste disposal, usage of porous conical bearings in lubrication technology, geophysics and energy related engineering problems. A good review of buoyancy driven boundary layer flows in Darcian fluid is given in Nield and Bejan [1]. When the Reynolds number is high enough for the Darcy flow model to breakdown, Pumb and Huenefeld [2] studied the fundamental problem of non-Darcy natural convection from heated vertical walls in a saturated porous medium. Later Bejan and Poulikakos [3] and Bejan [4], by dividing the flow regime into non-Darcy and intermediate regimes, studied the same problems using fluid inertia-buoyancy scaling and defined large Reynolds number-limit Rayleigh number. The non-similar boundary-layer equations resulting from the Forchheimer natural convection with power law wall variation were solved by Chen and Ho [5].

The transverse thermal dispersion effects will become important, and the analysis is dealt with at length in works by Plumb [6], Cheng [7], Hong and Tien

[8], Hong et al. [9], Cheng and Vortmeyer [10], Amiri and Vafai [11] etc. All these works confirm the importance of the thermal dispersion effect. Except for Cheng and Vortmeyer [10], all other works use the linear dependence of dispersion diffusivity on stream wise velocity. In order to correlate the available experimental data concerning the packed beds, Cheng and Vortmeyer [10] introduced a wall function term into the term of dispersion diffusivity.

The effect of viscous dissipation on natural convection in fluids has been studied by Gebhart [12] for power law vertical wall variation. He obtained a perturbation solution in terms of a parameter which could not be expressed in terms of either the Rayleigh number or the Prandtl number, and observed its increasing effect as the Prandtl number increases. Later Gebhart and Mollendor [13] obtained the similarity solution for the same problem when exponential wall temperature variation is used and a similar trend was observed. A comment was made by Fand and Brucker [14] that the effect of viscous dissipation might be significant in the case of natural convection in porous medium in connection with their experimental correlation for heat transfer in external flows. The validity of the comment was tested for the Darcy model by Fand et al. [15], both experimentally and analytically while estimating the heat transfer coefficient from a horizontal cylinder embedded in a saturated porous medium. Their mathematical analysis is confined to studying the dissipation effect using a steady, energy Equation, the basis of the equation is from the analogy given by Bejan [16] for the inclusion of viscous dissipation effects. The influence of viscous dissipation can be seen from the analogy given by Tucker and Dessenberger [17] to model the heat transfer

The effect of viscous dissipation on natural convection has been studied for some different cases including the natural convection from horizontal cylinder embedded in a porous media by Fand and Brucker [19] and Fand et al. [20]. They reported that the viscous dissipation may not be neglected in all cases of natural convection from horizontal cylinders and further, that the inclusion of a viscous dissipation term in porous medium may lead to more accurate correlation equations. This observation has been pointed out also by Murthy and Singh [21] for the natural convection flow along an isothermal vertical wall embedded in a porous medium. Recently, Nawaf H. Saeid and I.Pop [22] studied the viscous dissipation effects on free convection in a porous cavity.

II. MATHEMATICAL FORMULATION

A vertical annular cone of inner radius r_i and outer radius r_o as depicted by schematic diagram as shown in figure (A) is considered to investigate the heat transfer behavior in the presence of viscous dissipation.

The co-ordinate system is chosen such that the r-axis points towards the width and z-axis towards the height of the cone respectively. Because of the annular nature, two important parameters emerges, which are Cone angle (C_A) and Radius ratio (R_r) of the annulus. They are defined

$$\text{as } C_A = \frac{H_t}{r_0 - r_i}, \quad R_r = \frac{r_0 - r_i}{r_i}$$

Where H_t is the height of the cone.

The inner surface of the cone is maintained at isothermal temperature T_h and outer surface is at ambient temperature T_∞ . It may be noted that, due to axisymmetry, only a section of the annulus is sufficient for analysis purpose. The horizontal surfaces of the vertical annular cone are considered adiabatic.

The flow inside the porous medium is assumed to obey Darcy law and there is no phase change of fluid. The properties of the fluid and porous medium are homogeneous, isotropic and constant except variation of fluid density with temperature. The fluid and porous medium are in thermal equilibrium with these assumptions, the governing equations are given by

Continuity Equation:
$$\frac{\partial(ru)}{\partial r} + \frac{\partial(rw)}{\partial z} = 0 \quad (2.1)$$

Energy equation:
$$u \frac{\partial T}{\partial r} + w \frac{\partial T}{\partial z} = \alpha \left(\frac{1}{r} \frac{\partial}{\partial r} \left(r \frac{\partial T}{\partial r} \right) + \frac{\partial^2 T}{\partial z^2} \right) + \frac{\mu}{K(\rho C_p)_f} (u^2 + w^2) \quad (2.7)$$

The continuity equation (2.1) can be satisfied by introducing the stream function ψ as

$$u = -\frac{1}{r} \frac{\partial \psi}{\partial z} \quad (2.8)$$

$$w = \frac{1}{r} \frac{\partial \psi}{\partial r} \quad (2.9)$$

The corresponding dimensional boundary conditions are

at $r = r_i$, $T = T_w$, $\psi = 0$ (12.10a)

at $r = r_o$, $T = T_\infty$, $\psi = 0$ (2.10b)

(except at $z = 0$)

The new parameters arising due to cylindrical co-ordinates system are

Non-dimensional Radius
$$\bar{r} = \frac{r}{L} \quad (2.11a)$$

The velocity in r and z directions can be described by Darcy law as

Velocity in horizontal direction
$$u = \frac{-K}{\mu} \frac{\partial p}{\partial z} \quad (2.2)$$

Velocity in vertical direction

$$w = \frac{-K}{\mu} \left(\frac{\partial p}{\partial z} + \rho g \right) \quad (2.3)$$

The permeability K of porous medium can be expressed as Bejan [24]

$$K = \frac{D_p^2 \phi^3}{180(1 - \phi)^2} \quad (2.4)$$

The variation of density with respect to temperature can be described by Boussinesq approximation as $\rho = \rho_\infty [1 - \beta_T (T - T_\infty)]$ (2.5)

Momentum Equation:
$$\frac{\partial w}{\partial r} - \frac{\partial u}{\partial z} = \frac{gK\beta}{\nu} \frac{\partial T}{\partial r} \quad (2.6)$$

Non-dimensional Height
$$\bar{z} = \frac{z}{L} \quad (2.11b)$$

Non-dimensional stream function
$$\bar{\psi} = \frac{\psi}{\alpha L} \quad (2.11c)$$

Non-dimensional Temperature
$$\bar{T} = \frac{(T - T_\infty)}{(T_w - T_\infty)} \quad (2.11d)$$

Rayleigh number
$$Ra = \frac{g\beta_T \Delta T K L}{\nu \alpha} \quad (2.11e)$$

Viscous dissipation parameter
$$\varepsilon = \frac{\alpha u}{\Delta T K \rho C_p} \quad (2.11f)$$

The non-dimensional equations for the heat transfer in vertical cone are

Momentum equation:
$$\frac{\partial^2 \bar{\psi}}{\partial \bar{z}^2} + \bar{r} \left(\frac{1}{\bar{r}} \frac{\partial \bar{\psi}}{\partial \bar{r}} \right) = \bar{r} Ra \frac{\partial \bar{T}}{\partial \bar{r}} \quad (2.12)$$

Energy equation

$$\frac{1}{r} \left[\frac{\partial \bar{\psi}}{\partial r} \frac{\partial \bar{T}}{\partial z} - \frac{\partial \bar{\psi}}{\partial z} \frac{\partial \bar{T}}{\partial r} \right] = \left(\frac{1}{r} \frac{\partial}{\partial r} \left(r \frac{\partial \bar{T}}{\partial r} \right) + \frac{\partial^2 \bar{T}}{\partial z^2} \right) + \varepsilon \left[\left(\frac{1}{r} \frac{\partial \bar{\psi}}{\partial r} \right)^2 + \left(\frac{1}{r} \frac{\partial \bar{\psi}}{\partial z} \right)^2 \right] \tag{2.13}$$

The corresponding non-dimensional boundary conditions are

$$\text{at } \bar{r} = \bar{r}_i, \quad \bar{T} = 1, \quad \bar{\psi} = 0 \tag{2.14a}$$

$$\text{at } \bar{r} = \bar{r}_o, \quad \bar{T} = 0, \quad \bar{\psi} = 0 \tag{2.14b}$$

III. SOLUTION OF GOVERNING EQUATIONS

Applying Galerkin method to momentum equation (2.12) yields:

$$\{R^e\} = - \int_V N^T \left(\frac{\partial^2 \bar{\psi}}{\partial z^2} + r \frac{\partial}{\partial r} \left(\frac{1}{r} \frac{\partial \bar{\psi}}{\partial r} \right) - r Ra \frac{\partial \bar{T}}{\partial r} \right) dV \tag{3.1}$$

$$\{R^e\} = - \int_A N^T \left(\frac{\partial^2 \bar{\psi}}{\partial z^2} + r \frac{\partial}{\partial r} \left(\frac{1}{r} \frac{\partial \bar{\psi}}{\partial r} \right) - r Ra \frac{\partial \bar{T}}{\partial r} \right) 2\pi r dA \tag{3.2}$$

where R^e is the residue. Considering individual terms of equation (3.2)

$$\frac{\partial}{\partial r} \left([N^T] \frac{\partial \bar{\psi}}{\partial r} \right) = [N^T] \frac{\partial^2 \bar{\psi}}{\partial r^2} + \frac{\partial [N^T]}{\partial r} \frac{\partial \bar{\psi}}{\partial r} \tag{3.3}$$

Thus,
$$\int_A N^T \frac{\partial^2 \bar{\psi}}{\partial r^2} dA = \int_A \frac{\partial}{\partial r} \left([N^T] \frac{\partial^2 \bar{\psi}}{\partial r^2} \right) 2\pi r dA - \int_A \frac{\partial [N^T]}{\partial r} \frac{\partial \bar{\psi}}{\partial r} dA \tag{3.4}$$

The first term on right hand side of equation (3.4) can be transformed into surface by the application of Greens theorem and leads to inter-element requirement at boundaries of an element. The boundary conditions are incorporated in the force vector.

Let us consider that the variable to be determined in the triangular area as "T" The polynomial function for "T" can be expressed as $T = \alpha_1 + \alpha_2 r + \alpha_3 z$ (3.5)

The variable T has the value T_i, T_j & T_k at the nodal position i, j & k of the element. The r and z coordinates at these points are r_i, r_j, r_k and z_i, z_j, z_k respectively.

$$\text{Since } T = N_i T_i + N_j T_j + N_k T_k \tag{3.6}$$

Where N_i, N_j & N_k are shape functions given by

$$N_m = \frac{a_m + b_m r + c_m z}{2A} \tag{3.7}$$

Making use of (3.7) gives
$$\int_A N^T \frac{\partial^2 \bar{T}}{\partial z^2} 2\pi r dA = - \int_A \frac{\partial N^T}{\partial r} \frac{\partial N}{\partial r} \left\{ \begin{matrix} \bar{\psi}_1 \\ \bar{\psi}_2 \\ \bar{\psi}_3 \end{matrix} \right\} dA \tag{3.8}$$

Substitution of (3.7) into (3.8) gives

$$= \frac{1}{(2A)^2} \int_A \begin{bmatrix} b_1 \\ b_2 \\ b_3 \end{bmatrix} [b_1 b_2 b_3] \begin{bmatrix} \bar{\psi}_1 \\ \bar{\psi}_2 \\ \bar{\psi}_3 \end{bmatrix} 2\Pi r dA = -\frac{2\Pi R}{4A} \begin{bmatrix} b_1^2 & b_1 b_2 & b_1 b_3 \\ b_1 b_2 & b_2^2 & b_2 b_3 \\ b_1 b_3 & b_2 b_3 & b_3^2 \end{bmatrix} \begin{bmatrix} \bar{\psi}_1 \\ \bar{\psi}_2 \\ \bar{\psi}_3 \end{bmatrix} \quad (3.9)$$

Similarly,

$$\int_A N^T \frac{\partial^2 \bar{\psi}}{\partial z^2} 2\Pi r dA = -\frac{2\Pi R}{4A} \begin{bmatrix} c_1^2 & c_1 c_2 & c_1 c_3 \\ c_1 c_2 & c_2^2 & c_2 c_3 \\ c_1 c_3 & c_2 c_3 & c_3^2 \end{bmatrix} \begin{bmatrix} \bar{\psi}_1 \\ \bar{\psi}_2 \\ \bar{\psi}_3 \end{bmatrix} \quad (3.10)$$

The third term of equation (3.2) gives

$$\int_A N^T r Ra \frac{\partial \bar{T}}{\partial r} 2\Pi r dA = Ra \int_A N^T r \frac{\partial \bar{T}}{\partial r} 2\Pi r dA \quad (3.11)$$

Since $M_1 = N_1, M_2 = N_2, M_3 = N_3$ Replacing the shape functions in the above
 Where $M_1, M_2,$ and M_3 are the area ratios of the equation (3.11) gives
 triangle and N_1, N_2 and N_3 are the shape functions.

$$\int_A N^T r Ra \frac{\partial \bar{T}}{\partial r} 2\Pi r dA = r Ra \int_A \begin{bmatrix} M_1 \\ M_2 \\ M_3 \end{bmatrix} \frac{\partial(N)}{\partial r} \begin{bmatrix} \bar{T}_1 \\ \bar{T}_2 \\ \bar{T}_3 \end{bmatrix} 2\Pi r dA \quad (3.12)$$

$$= Ra \frac{A}{3} \begin{bmatrix} 1 \\ 1 \\ 1 \end{bmatrix} \frac{2\Pi R^2}{2A} [b_1 + b_2 + b_3] \begin{bmatrix} \bar{T}_1 \\ \bar{T}_2 \\ \bar{T}_3 \end{bmatrix} = \frac{2\Pi R^2 Ra}{6} \begin{Bmatrix} b_1 \bar{T}_1 + b_2 \bar{T}_2 + b_3 \bar{T}_3 \\ b_1 \bar{T}_1 + b_2 \bar{T}_2 + b_3 \bar{T}_3 \\ b_1 \bar{T}_1 + b_2 \bar{T}_2 + b_3 \bar{T}_3 \end{Bmatrix} \quad (3.13)$$

Now Momentum equation leads to

$$\frac{2\Pi R}{4A} \begin{Bmatrix} b^2 & b_1 b_2 & b_1 b_3 \\ b_1 b_2 & b_2^2 & b_2 b_3 \\ b_1 b_3 & b_2 b_3 & b_3^2 \end{Bmatrix} + \begin{bmatrix} c_1^2 & c_1 c_2 & c_1 c_3 \\ c_1 c_2 & c_2^2 & c_2 c_3 \\ c_1 c_3 & c_2 c_3 & c_3^2 \end{bmatrix} \begin{Bmatrix} \bar{\psi}_1 \\ \bar{\psi}_2 \\ \bar{\psi}_3 \end{Bmatrix} + \frac{2\Pi R^2 Ra}{6} \begin{Bmatrix} b_1 \bar{T}_1 + b_2 \bar{T}_2 + b_3 \bar{T}_3 \\ b_1 \bar{T}_1 + b_2 \bar{T}_2 + b_3 \bar{T}_3 \\ b_1 \bar{T}_1 + b_2 \bar{T}_2 + b_3 \bar{T}_3 \end{Bmatrix} = 0 \quad (3.14)$$

Which is in the form of the stiffness matrix $[K_s] \{\psi\} = \{f\}$

Similarly application of Galerkin method to Energy equation gives

$$\{R^e\} = -\int_A N^T \left[\frac{1}{r} \left(\frac{\partial \bar{\psi}}{\partial r} \frac{\partial \bar{T}}{\partial z} - \frac{\partial \bar{\psi}}{\partial z} \frac{\partial \bar{T}}{\partial r} \right) - \left[\frac{1}{r} \frac{\partial}{\partial r} \left(-\frac{\partial \bar{T}}{\partial r} + \frac{\partial^2 \bar{T}}{\partial z^2} \right) \right] - \varepsilon \left[\frac{1}{r} \left(\frac{\partial \bar{\psi}}{\partial r} \right)^2 + \left(\frac{1}{r} \frac{\partial \bar{\psi}}{\partial z} \right)^2 \right] \right] 2\Pi r dA \quad (3.15)$$

Considering the terms individually of the energy equation and following the same above steps. We get the stiffness matrix of energy equation as:

$$\left[\frac{2\Pi}{12A} \begin{bmatrix} c_1 \bar{\psi}_1 + c_2 \bar{\psi}_2 + c_3 \bar{\psi}_3 \\ c_1 \bar{\psi}_1 + c_2 \bar{\psi}_2 + c_3 \bar{\psi}_3 \\ c_1 \bar{\psi}_1 + c_2 \bar{\psi}_2 + c_3 \bar{\psi}_3 \end{bmatrix} [b_1, b_2, b_3] - \frac{2\Pi}{12A} \begin{bmatrix} b_1 \bar{\psi}_1 + b_2 \bar{\psi}_2 + b_3 \bar{\psi}_3 \\ b_1 \bar{\psi}_1 + b_2 \bar{\psi}_2 + b_3 \bar{\psi}_3 \\ b_1 \bar{\psi}_1 + b_2 \bar{\psi}_2 + b_3 \bar{\psi}_3 \end{bmatrix} [c_1, c_2, c_3] \right] \begin{bmatrix} \bar{T}_1 \\ \bar{T}_2 \\ \bar{T}_3 \end{bmatrix}$$

$$\begin{aligned}
 & + \frac{2\Pi R}{4A} \left\{ \begin{bmatrix} b_1^2 & b_1 b_2 & b_1 b_3 \\ b_1 b_2 & b_2^2 & b_2 b_3 \\ b_1 b_3 & b_2 b_3 & b_3^2 \end{bmatrix} \begin{bmatrix} \bar{T}_1 \\ \bar{T}_2 \\ \bar{T}_3 \end{bmatrix} + \begin{bmatrix} c_1^2 & c_1 c_2 & c_1 c_3 \\ c_1 c_2 & c_2^2 & c_2 c_3 \\ c_1 c_3 & c_2 c_3 & c_3^2 \end{bmatrix} \begin{bmatrix} \bar{T}_1 \\ \bar{T}_2 \\ \bar{T}_3 \end{bmatrix} \right\} \\
 & + \frac{2\Pi A \epsilon}{12r} \left\{ \begin{bmatrix} 1 \\ 1 \\ 1 \end{bmatrix} \left[b_1 \bar{\psi}_1 + b_2 \bar{\psi}_2 + b_3 \bar{\psi}_3 \right]^2 + \begin{bmatrix} 1 \\ 1 \\ 1 \end{bmatrix} \left[c_1 \bar{\psi}_1 + c_2 \bar{\psi}_2 + c_3 \bar{\psi}_3 \right]^2 \right\} = 0 \quad (3.16)
 \end{aligned}$$

IV. RESULTS AND DISCUSSION

Results are obtained in terms of the average Nusselt number (\bar{Nu}) at hot wall for various parameters

such as Rayleigh number (Ra), Radius ratio (R_r), Cone angle (C_A) and Viscous dissipation (ϵ) when heat is supplied to the vertical annular cone.

The average Nusselt number (\bar{Nu}), is given by $\bar{Nu} = \int_0^z \left(\frac{\partial T}{\partial r} \right)$

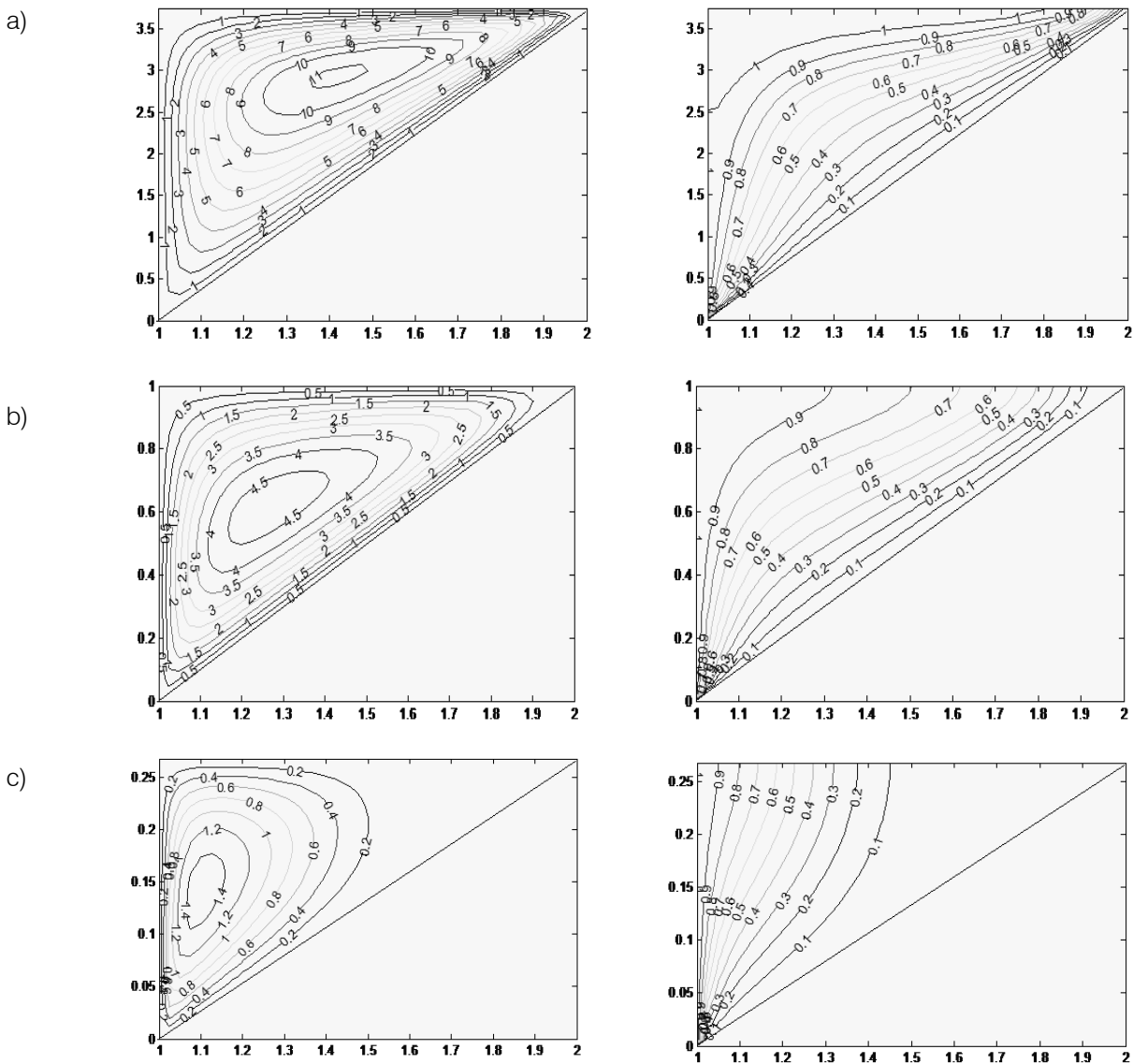


Figure 1 : Streamlines (left) and Isotherms (Right) for $Ra=100, R_r=1, \epsilon=0.01$

a) $C_A = 15$ b) $C_A = 45$ c) $C_A = 75$

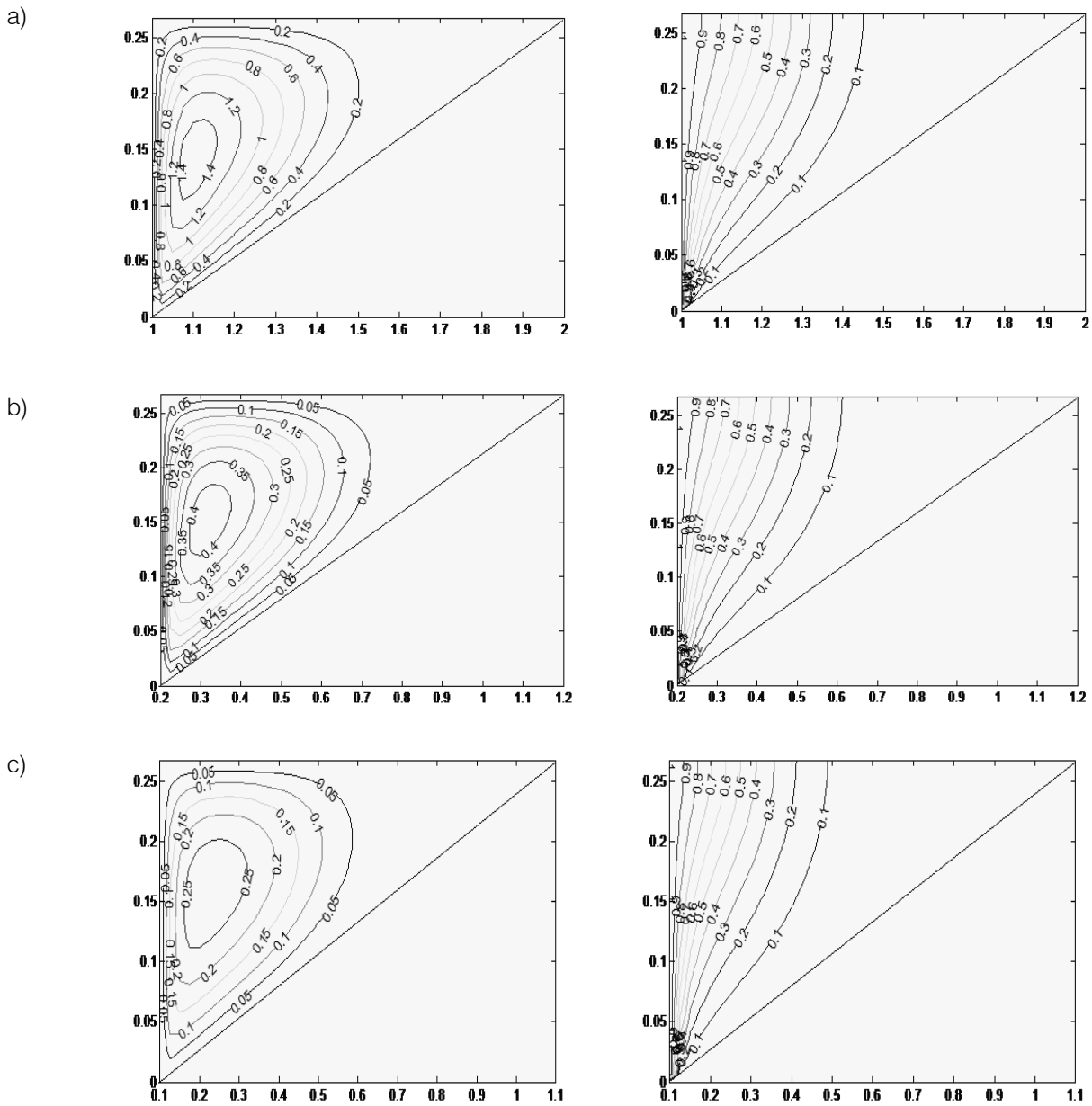
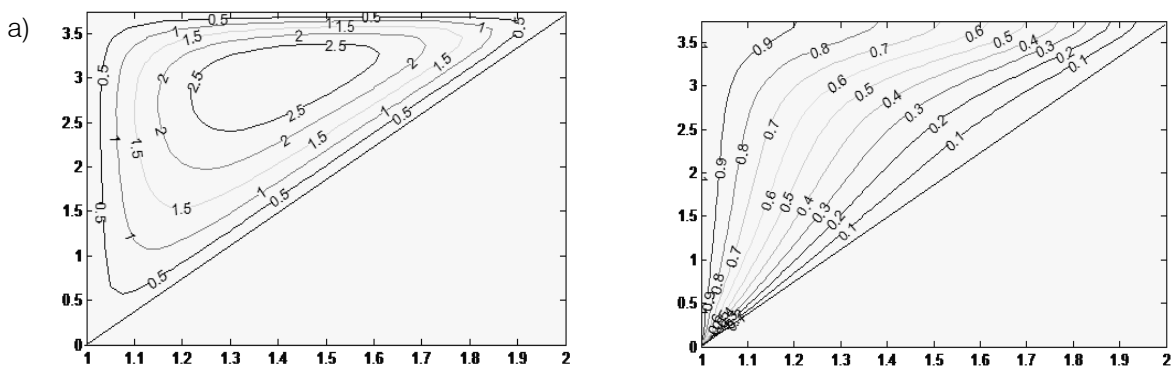


Figure 2 : Streamlines (left) and Isotherms (Right) for $Ra=100$, $C_A=75$, $\epsilon=0.01$ $R_r=1$ b) $R_r=5$ c) $R_r=10$ a)



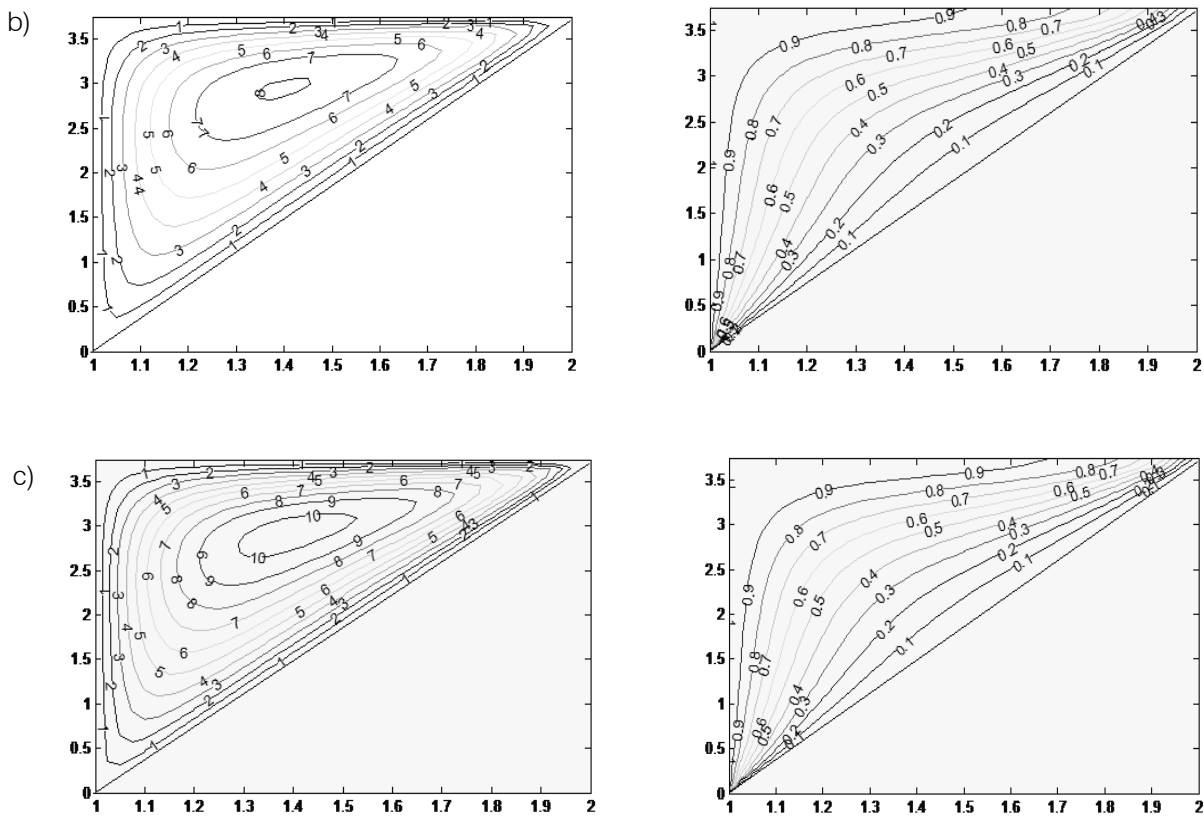


Figure 4 : Streamlines (left) and Isotherms (Right) for $\epsilon=0.003, C_A = 15, R_r=1$

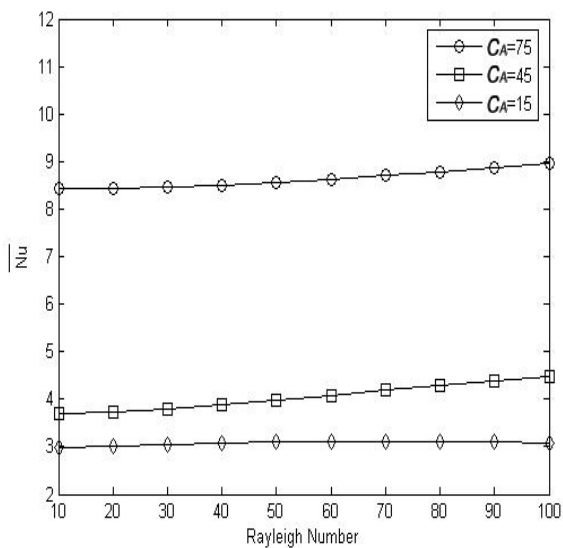


Figure 5 : \overline{Nu} variations with Ra at hot surface for different values of C_A at $R_r=1, \epsilon=0.003$

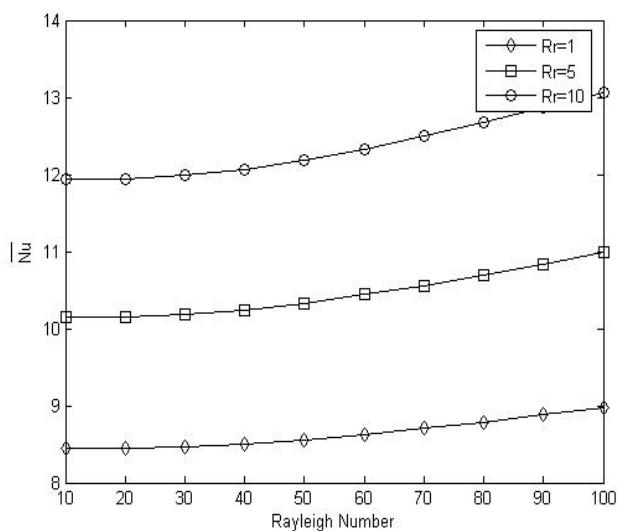


Figure 6 : \overline{Nu} variations with Ra at hot surface for different values of R_r at $C_A=75, \epsilon=0.01$

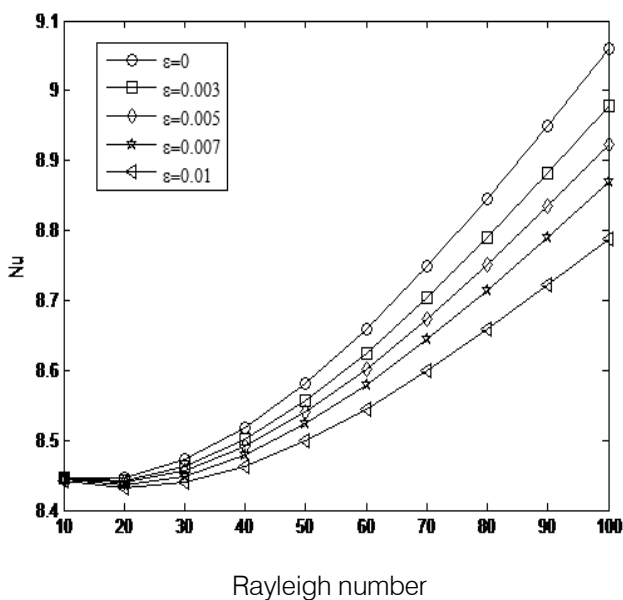


Figure 7 : \overline{Nu} variations with Ra at hot surface for different values of ϵ at $C_A = 75, R_r = 1$

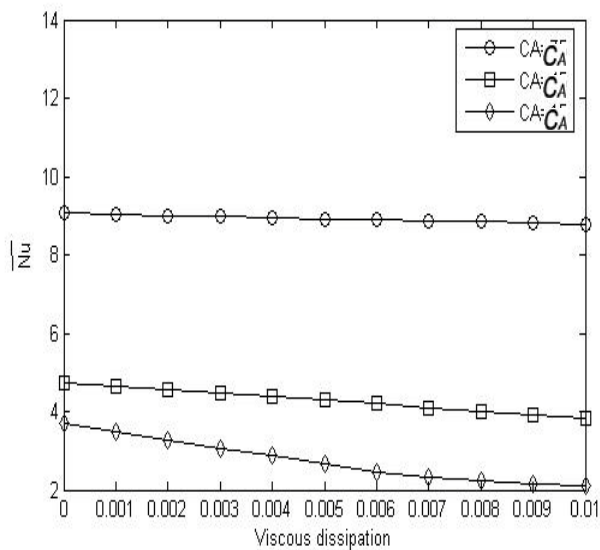


Figure 8 : \overline{Nu} variations with ϵ at hot surface for different values of C_A at $R_r = 1, Ra = 100$

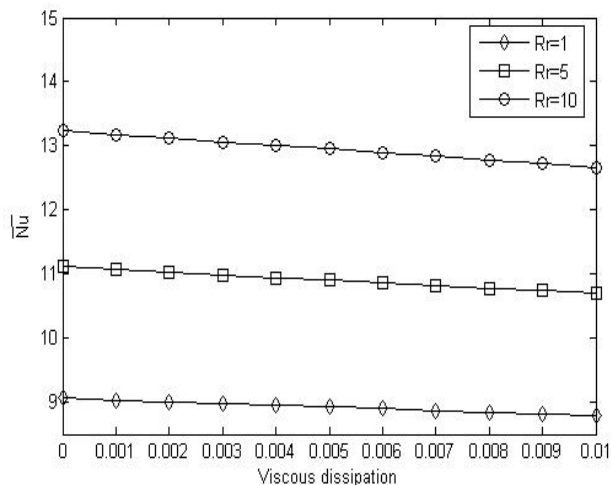


Figure 9 : \overline{Nu} variations with ϵ at hot surface for different values of R_r at $C_A = 75, Ra = 100$

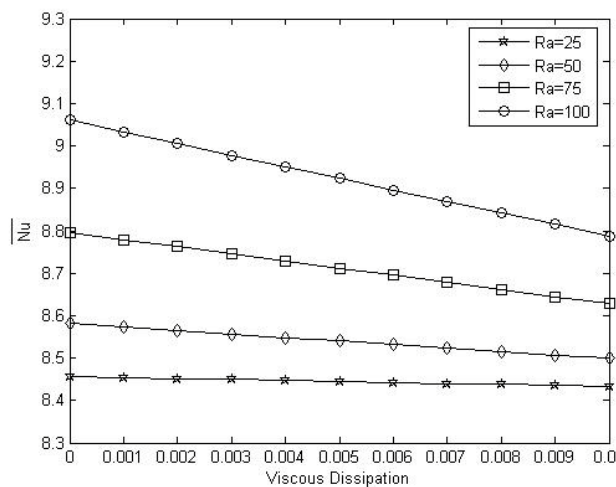


Figure 10 : \overline{Nu} variations with ϵ at hot surface for different values of Ra at $C_A = 75, R_r = 1$

Fig.1 (a-c) shows the streamlines and isothermal lines distribution inside the porous medium with respect of various values of Cone angle (C_A) at $Ra = 100, R_r = 1,$ and $\epsilon = 0.01$. The stream lines and isothermal lines move away from the cold wall and reach nearer to the hot wall as Cone angle (C_A) increase. It can be seen that the thickness of thermal boundary layer decreases with increasing Cone angle (C_A). The isothermal lines are evenly distributed between the two vertical surfaces at smaller Cone angle (C_A). The magnitude of stream lines decrease with increasing Cone angle (C_A) and occupies only half of the domain.

Fig.2 (a-c) illustrates the streamlines and isothermal lines distribution inside the porous medium for various values of Radius ratio (R_r) at $Ra = 100, C_A = 75$ and $\epsilon = 0.01$. It is seen that the magnitude of streamlines decreases with the increase in Radius ratio (R_r). This happens due to the reason that at high Rayleigh number (Ra) with the viscous dissipation

parameter (ϵ), leads to more fluid movement at the hot wall of the cone. The isothermal lines tend to move towards the hot surface of the cone as the Radius ratio (R_r) increases, because the thermal boundary layer becomes thicker.

Fig.3 (a-c) illustrates the streamlines and isothermal lines distribution inside the porous medium for various values of viscous dissipation parameter (ϵ) at $Ra=100$, $C_A = 75$ and $R_r = 1$. For increasing the values of viscous dissipation parameter (ϵ) no change of has been observed in the formation and occupation of the domain by streamlines and isothermal lines only half of the domain is covered with streamlines and isothermal lines.

Fig.4 (a-c) shows the streamlines and isothermal lines distribution inside the porous medium of the vertical annular cone for various values of Rayleigh number (Ra) at $\epsilon = 0.003$, $C_A = 15$ and $R_r = 1$. As the value of Rayleigh number (Ra) increases the magnitude of stream lines also increases. This is due to the reason that the increased Rayleigh number (Ra) promotes the fluid movements due to higher buoyancy force, which in term allows the convection heat transfer at lower partition of the hot wall of the vertical annular cone.

Fig.5 demonstrates the effect of Rayleigh number (Ra) and Cone angle (C_A) on the average Nusselt number (\overline{Nu}). This figure corresponds to the values $R_r = 1$ and $\epsilon = 0.003$. It is found that the average Nusselt number (\overline{Nu}) increases with increase in Rayleigh number (Ra) and Cone angle (C_A). For a given Rayleigh number (Ra), the difference between the average Nusselt number (\overline{Nu}) at two difference values of Cone angle (C_A) increase with Cone angle (C_A). For instance the average Nusselt number (\overline{Nu}) increased by 23% when Cone angle (C_A) is increased from 15 to 45 at $Ra = 10$. However the average Nusselt number (\overline{Nu}) increased by 45% when Cone angle (C_A) is increased from 15 to 45 at $Ra = 100$. This difference becomes more as the Rayleigh number (Ra) increases for particular value of Cone angle (C_A).

Fig.6 illustrates the effect of Rayleigh number (Ra) on the average Nusselt number (\overline{Nu}) for various values of Radius ratio (R_r). This figure corresponds to the values of $C_A = 75$, $\epsilon = 0.01$. The average Nusselt number (\overline{Nu}) at hot wall of the vertical annular cone increases with increase in Radius ratio (R_r) and Rayleigh number (Ra). The average Nusselt number (\overline{Nu}) is increased by 41% at $Ra = 10$. Whereas at $Ra = 100$, it is found to be 45% with increase in Radius ratio (R_r) from 1 to 5.

Fig.7 demonstrates the effect of Rayleigh number (Ra) and viscous dissipation (ϵ) on the average

Nusselt number (\overline{Nu}). This figure corresponds to the values $C_A = 75$, $R_r = 1$. It can be seen that the effect of viscous dissipation parameter (ϵ) is to reduce the average Nusselt number (\overline{Nu}) at hot wall. The temperature difference near the hot wall increases with increase in viscous dissipation parameter (ϵ). This happens due to the reason that the viscous dissipation leads to local heat generation, which increases the temperature in the porous medium. As the temperature of hot wall T_w is constant, the increased temperature of porous medium reduces the temperature difference between the hot wall and the near region. Due to this reason the heat transfer from hot wall to the porous medium increases which results in increasing the average Nusselt number (\overline{Nu}). The effect of viscous dissipation (ϵ) is higher at the lower values of Rayleigh number (Ra) as compared to the higher values of Rayleigh number (Ra). At $Ra = 10$, the average Nusselt number (\overline{Nu}) decreased by 4% when viscous dissipation parameter (ϵ) is increased 0 to 0.01. Whereas the corresponding reduction in the average Nusselt number (\overline{Nu}) at $Ra = 100$ is found to be 18%. The effect of viscous dissipation becomes more dominant at high Rayleigh number (Ra) as compared to lower Rayleigh number (Ra).

Fig.8 illustrates the effect of viscous dissipation parameter (ϵ) on the average Nusselt number (\overline{Nu}) for various values of cone angle (C_A). This figure is obtained for $R_r=1$, $Ra=100$. It can be seen that the average Nusselt number (\overline{Nu}) decreases with the increase in viscous dissipation parameter (ϵ). When there is no viscous dissipation then the average Nusselt number (\overline{Nu}) at hot wall always increases with increase Cone angle (C_A). This happens due to reason that higher Cone angle (C_A) leads to high buoyancy force and thus faster fluid movement. This faster fluid movement enhances the local friction between fluid and solid matrix thus increasing the local heat generation, which in turn reduces the average Nusselt number (\overline{Nu}). When there is no viscous dissipation parameter (ϵ), there is a decrease in the average Nusselt number (\overline{Nu}). Which is found to be 26.3 %, when Cone angle (C_A) increases from 15 to 45. At $\epsilon = 0.01$, it is found that there is a decrease in the average Nusselt number (\overline{Nu}) by 46.2%. This shows that there is a decrease in the average Nusselt number (\overline{Nu}) as the viscous dissipation parameter (ϵ) increases.

Fig.9 illustrates the effect of Viscous dissipation parameter (ϵ) on the average Nusselt number (\overline{Nu}) for

various values of Radius ratio (R_r). This figure is obtained for $C_A = 75$, $Ra = 100$. It can be seen that the average Nusselt number (\overline{Nu}) decreases with the increase in viscous dissipation parameter (ϵ). When there is no viscous dissipation (ϵ), at $\epsilon = 0$, the average Nusselt number (\overline{Nu}) at hot wall always increase with increase in Radius ratio (R_r). Whereas at $\epsilon = 0.005$, the average Nusselt number (\overline{Nu}) decreases as R_r is reduced. At $\epsilon = 0.01$, the average Nusselt number (\overline{Nu}) always decreases with increase in Radius ratio (R_r). This happens due to the reason that higher Radius ratio (R_r) leads to high buoyancy force and this faster fluid movement. This faster fluid movement enhances the local friction between fluid and solid matrix thus increasing the local heat generation.

Fig.10 illustrates the effect of Viscous dissipation parameter (ϵ) on the average Nusselt number (\overline{Nu}) for various values of Rayleigh number (Ra). This figure is obtained for $C_A = 75$, $R_r=1$. It can be seen that the average Nusselt number (\overline{Nu}) decreases with the increase in viscous dissipation parameter (ϵ). At $Ra=25$, the average Nusselt number (\overline{Nu}) is linear, whereas at $Ra=100$, at lower viscous dissipation parameter (ϵ), the average Nusselt number (\overline{Nu}) increases and decreases with higher viscous dissipation parameter (ϵ). This happens due to the reason that higher Rayleigh number (Ra) leads to high buoyancy force and thus faster fluid movement. This faster fluid movement enhances the local friction between fluid and social matrix thus increasing the local heat generation.

REFERENCES RÉFÉRENCES REFERENCIAS

- Nield, D.A. and Bejan, A., "convection in porous media". Springer verlag, New York (1992).
- Plumb, O. and Huenefeld, J.C., "Non-Darcy natural convection from heated surfaces in saturated porous medium". Int. J. of Heat and Mass Transfer, Vol (24), pp.765-768 (1981).
- Bejan, A. and Poulidakos, D., "The Non - Darcy regime, for vertical boundary layer natural convection in a porous medium". Int. J. of Heat and Mass Transfer, Vol (27), pp.717-722(1984).
- Bejan, A., "The basic scales of natural convection heat and mass transfer in fluids and fluid saturated porous media". Int. comm. in heat and mass Transfer, Vol (14), pp.107-123 (1987).
- Chen, K.S. and Ho, J.R., "Effects of flow inertia on vertical natural convection in saturated porous media", Int. J. of Heat and mass Transfer, Vol (29), pp.753-759 (1986).
- Plumb, O., "The effect of thermal dispersion on heat transfer in packed bed boundary layers". Proceedings of first ASME and JSME thermal Engineering Joint conference, Vol (2), pp.17-21 (1983).
- Cheng, P., "Thermal dispersion effects in Non-Darcian convective flows in a saturated porous medium". Letters to Heat & mass Transfer, Vol (8), pp.267-270 (1981).
- Heng, J.T. and Tien, C.L., "Analysis of thermal dispersion effect on vertical plate natural convection in porous media". Int. J. of Heat and Mass Transfer, Vol (30), pp. 143-150 (1987).
- Hong, J.T., Yamada, Y. and Tien, C.L., "Effects of non -Darcian and non-uniform porosity on vertical plate natural convection in porous media". J. of Heat and Mass Transfer, Vol (109), pp.356-361 (1987).
- Cheng. P. and Vortmeyer, D., "Transverse thermal dispersion and wall channelling in a packed bed with forced convective flow". Chemical Engineering Science, Vol (43), pp.2523-2532 (1988).
- Amiri, A. and Vafai, K., "Analysis of dispersion effects and non-thermal equilibrium, non -Darcian, variable porosity incompressible flow through porous media". Int. J. of Heat and Mass Transfer, Vol (37), pp. 939-954 (1994).
- Gebhart, B., "Effects of viscous dissipation in natural convection". J. of fluid Mechanics, Vol (14), pp.225-235 (1962).
- Gebhart, B. and Mollendorf J., "Viscous dissipation in external natural convection flows". Journal of fluid Mechanics, Vol(38), pp.97-107 (1969).
- Fand, R.M. and Brucker, J., "A correlation for heat transfer by natural convection from horizontal cylinders that accounts for viscous dissipation". Int. J. of Heat and Mass Transfer, Vol (26), pp.709-726 (1983).
- Fand, R.M., Steinberger, T.E. and Cheng, P. "Natural convection heat transfer from a horizontal cylinder embedded in a porous medium". Int. J. of Heat and Mass Transfer, Vol (29), pp.119-133 (1986).
- Bejan, A., "Convection Heat Transfer", wiley, New York pp.343 - 416 (1984).
- Tucker. CL, and Dessenberger. RB. "Governing equations for flow and heat transfer in stationary fiber beds. In flow and Rheology in polymer composites manufacturing, ed. SG. Advani. Elsevier Science, Amsterdam, pp.257-323, (1994).
- Nakayama, A., and Pop, I., "Free convection over a non-isothermal body in a porous medium with viscous dissipation". Int. comm. in Heat and Mass Transfer, Vol (16), pp.173-180 (1989).
- R.M. Fand, J. Brucker, A correlation for heat transfer by natural convection from horizontal cylinders that accounts for viscous dissipation, Int. J. of Heat and Mass Transfer, Vol (26), pp.709-726, (1983).

20. R. M. Fand, T. E. Steinberger and P. Cheng, "Natural Convection Heat Transfer from Horizontal Cylinder embedded in a Porous medium", *Int. J. of Heat and Mass Transfer*, Vol. 29, no. 1, pp. 119-133(1986).
21. P. V. S. N. Murthy and P. Singh, "The effect of viscous dissipation on non-Darcy natural convective regime" *Int. J. Heat and Mass Transfer*, Vol (40) pp. 1251-1260, (1997).
22. Nawaf H. Saeid and I. Pop., "Viscous dissipation effects on free convection in a porous cavity", *Intro. Comm. Heat mass Transfer*, Vol (31), pp.723-732, (2004).
23. S.V. Patankar, *Numerical Heat Transfer and fluid flow*, Hemisphere publishing corporation, Washington (1980).
24. A.Bejan "convective Heat Transfer", 2nd edition, New York, John Wiley & Sons, (1995).
25. R.W. Lewis, P. Nithiarasu and K.N. Seetharamu, "Fundamentals of the finite element method for heat and fluid flow", John Wiley and sons, Chichester (2004).
26. L.T. Segerland, "Applied Finite Element Analysis", John Wiley and Sons, New York (1982).